Genomic epidemiology of a 2023–2024 Oropouche virus disease outbreak in Iquitos, Peru: descriptive analysis of a case control study for acute febrile illness

Maribel Paredes Olortegui,[a] Francesca Schiaffino,[b,c] Pablo Peñataro Yori,[a,b] Josh M. Colston,[b] Evangelos Mourkas,[d] Wagner V. Shapiama Lopez,[a] Tackeshy N. Pinedo Vasquez,[a] Paul F. Garcia Bardales,[a] Thomas G. Flynn,[b] Cesar Ramal-Asayag,[e,f] Holly R. Hughes,[g] Emily Davis,[g] Brandy J. Russell,[g] Aaron C. Brault,[g] Yuri A. Alegre Palomino,[h] Cesar V. Munayco,[i] Jie Liu,[j] Eric Houpt,[b] Ben Pascoe,[k] Kerry K. Cooper,[l] Craig T. Parker,[m] and Margaret N. Kosek[a,b,*]

[a]Asociación Benéfica Prisma, Iquitos, Peru
[b]Division of Infectious Diseases and International Health, School of Medicine, University of Virginia, VA, USA
[c]Faculty of Veterinary Medicine, Universidad Peruana Cayetano Heredia, San Martin de Porres, Lima, Peru
[d]Department of Medical Sciences, Uppsala University, Sweden
[e]School of Human Medicine, Universidad Nacional de la Amazonia Peruana, Iquitos, Peru
[f]Research Laboratory of Infectious and Tropical Diseases, Hospital Regional de Loreto "Felipe Santiago Arriola Iglesias", Iquitos, Peru
[g]Arboviral Diseases Branch, Division of Vector-borne Diseases, US Center for Disease Control and Prevention, Fort Collins, CO, USA
[h]Gerencia Regional de Salud, Gobierno Regional de Loreto, Loreto, Peru
[i]Centro Nacional de Epidemiologia, Prevención y Control de Enfermedades, Ministerio de Salud, Peru
[j]School of Public Health, Qingdao University, Qingdao, China
[k]Centre for Genomic Pathogen Surveillance, Big Data Institute, University of Oxford, UK
[l]School of Animal and Comparative Biomedical Sciences, University of Arizona, Tucson, AZ, USA
[m]Agricultural Research Service, U.S. Department of Agriculture, Produce Safety and Microbiology Research Unit, Albany, CA, USA

The Lancet Regional Health - Americas 2026;56: 101413

Published Online xxx https://doi.org/10.1016/j.lana.2026.101413

Summary

Background Oropouche virus (OROV) is an emerging vector-borne pathogen endemic to the Americas, which causes acute febrile illness (AFI) in humans. Starting in late 2023, surges in OROV infections were reported across Latin America, including an outbreak in Iquitos, a city in the Eastern Peruvian Amazon, where RIVERA, an ongoing AFI surveillance program detected and characterized incident OROV cases.

Methods AFI cases presenting to health facilities were screened for OROV using PCR. OROV-positive subjects were compared to AFI OROV negative cases to describe the principal features of clinical disease. Genomes from OROV strains were sequenced and compared using phylogenetic analysis with those from extant samples isolated from other locations in the Americas.

Findings In early 2024, an 8.6% OROV-positivity rate (29 detections in 339 samples) in RIVERA subjects was recorded, a more than 20-fold increase compared with pre-outbreak levels. Illness was characterized by fever, arthralgia, myalgia and dysuria. Genome sequences from strains in this outbreak were phylogenetically distinct from those from a concurrent one in Brazil, but resembled strains from Colombia and Ecuador. The last common ancestor of outbreak strains from Peru and Brazil was 226 years prior to sampling, and that of Peru and Ecuador and Colombia approximately 10 and 8 years prior to sampling, respectively.

Interpretation Genomic analysis suggests that the current outbreak in South America is multifocal in origin and not the result of geographic spread from Brazil. An existing AFI surveillance program successfully documented the emergence and characterized the symptom profile of this emerging arboviral disease.

Funding CDC/HHS U01GH002270; NIH D43TW010913, K43TW012298, K01AI168493, 5T32AI007046-48.

*Corresponding author. Division of Infectious Diseases, International Health, and Public Health Sciences, University of Virginia, 345 Crispell Dr, Rm 2525, Charlottesville, VA, USA.
E-mail address: mkosek@virginia.edu (M.N. Kosek).

Disclaimer: This summary is available in Spanish in the Supplementary Materials.

Keywords: Arbovirus; Orthobunyavirus; Acute febrile illness

Research in context

Evidence before this study

A targeted review on the genomic epidemiology of Oropouche using the search terms "Oropouche" and genomic epidemiology" or "phylogenetic" or "molecular epidemiology" was conducted in PubMed and Embase through August 22, 2025 yielded 56 articles and signaled the paucity of information available regarding the transmission dynamics of Oropouche.

Added value of this study

Most epidemiologic studies documenting the emergence or temporal ecology of Oropouche were limited to regional or national spread of disease within a single country (Brazil), or among travelers returning from endemic countries and focused on the dissemination within a temporal scale limited to the present outbreak. This work documents the emergence of the Oropouche outbreak within an established surveillance system and used a comprehensive historical and geographic genomic analysis to discern the geographic origins of the outbreak in Loreto Peru in late 2023.

Implications of all the available evidence

The evidence implies that the recent outbreak in South America was the product of multifocal resurgence with limited regional dispersion rather than a focal emergence in a single country with subsequent wide geographic dispersion of a dominant lineage.

Introduction

Oropouche virus (OROV) is a significant vector-borne pathogen in Latin America, with half a million cases of illness reported in South America, Central America, and the Caribbean since its initial description in 1955.[1] Although periodic outbreaks have been well documented, the extent of each outbreak is poorly defined, likely due to the limited availability of diagnostics for a disease that is not clearly clinically differentiated from other etiologies of acute febrile illness (AFI). However, OROV infection and transmission have been documented clearly in the region since the late 1990s, and in Brazil between the 1970s and the 1980s.[2–4]

Orthbunyavirus oropoucheense is in the Simbu serogroup of the orthobunyaviruses which possess three RNA negative-sense genomic segments (L, M and S) that undergo reassortment, leading to related but distinct viruses, such as Iquitos,[5] Madre de Dios[6] and Perdões[7] viruses. Other human pathogenic orthobunyaviruses have been identified in the region of Loreto (such as the Itaya[8] and Bellavista[9] viruses), yet their overall burden, distribution, and epidemiology largely remain obscure. The most thoroughly implicated vector in experimental studies and field epidemiology in the urban cycle is *Culicoides paraensis*,[10] a midge species with a range extending from subtropical South America to well within the territory of the Southern United States. There is some evidence that the *Culex quinquefasciatus* mosquito is also involved in urban OROV transmission cycle, but vectorial capacity is much lower.[11] Wild vertebrate animals act as reservoir hosts for OROV, and the virus has been detected in sloths, non-human neotropical primates, and a rodent, while a variety of wild and domestic birds have been found to be seropositive.[3]

OROV disease manifests itself as clinically indistinguishable from other arboviral etiologies of AFI. The most common symptoms are fever, myalgia, and headache. However, neurological symptoms consistent with meningitis and encephalitis have also been reported as have hemorrhagic symptoms.[12] The risk factors for OROV disease are poorly characterized, however outbreaks tend to occur in the rainy season and areas of recent deforestation or forest fragmentation.[13] In prior epidemics, dispersion patterns are thought to result from human movement among or to urban localities with the potential urban vector *C. paraensis* is found.[14]

A surge in reported OROV disease cases in the Americas was detected in early 2024, with re-emergence documented in Brazil, Bolivia, Ecuador and Peru, autogenous cases in Cuba, Panama and the Dominican Republic and cases in returning travelers in the United States, Canady, Italy, Spain, and Germany.[15] The Pan American Health Organization (PAHO) issued an alert on February 2, 2024.[16] This article describes the clinical, epidemiological, and genomic findings of an outbreak of OROV disease in Iquitos, Loreto, Peru, lasting from December 1st, 2023 to August 31st, 2024 detected by an ongoing AFI surveillance study[17] and uses available regional sequences to trace the origin of the outbreak strain.

Methods

Study design and participant enrollment

The RIVERA study, a prospective health facility-based case–control study of AFI in Iquitos, Peru, was initiated in early 2021 and is ongoing. The design, enrollment procedures, and diagnostic details of RIVERA have been described.[17] Patients aged ten years or older from a homogenous mestizo population seeking care for AFI (cases) were enrolled, as well as age- and site-

matched controls with no AFI symptoms. Fifty case–control dyads were enrolled each month, to ensure statistical power to detect a five-fold change in the monthly prevalence of a given pathogen with a baseline prevalence of 1%, assuming 80% power and a 95% confidence level. The detection rate of approximately 1% is conservative and derived from regional studies showing this is the interepidemic prevalence of emerging infectious diseases such as OROV and Mayaro virus.[18]

Sample and data collection at baseline and early convalescence

Enrollees underwent a baseline clinical assessment, and contributed blood and nasopharyngeal samples, which were tested for a locally relevant panel of pathogens by reverse transcription polymerase chain reaction (RT-PCR) (Supplementary Figure S1). Clinical information collected at baseline included pre-existing diseases, clinical signs and symptoms in the prior two weeks, vital signs and anthropometric measurements. Demographic and epidemiologic information collected included age, sex, area of residence, travel in the past 15 days, presence of ectoparasites and animals in the home. Participant follow-up was carried out 21–28 days after enrollment. Field workers contacted cases and controls using instant messaging and visited their households to ascertain their health status.

Features of clinical disease

Descriptive statistics were calculated comparing baseline and clinical characteristics between OROV-positive and -negative AFI cases, using the Fisher's exact test (due to the small number of OROV-cases) for differences in proportions of categorical variables and t-tests for difference in means of continuous variables.

Sample processing and OROV diagnosis

Total nucleic acids (TNA) were extracted from whole blood samples using the High Pure Viral Nucleic Acid Large Volume Kit (Roche Life Science, Indianapolis, IN) as instructed by manufacturers. TNA from whole blood samples was tested for OROV using TaqMan array cards (Thermo Fisher Scientific, Waltham, MA). The pathogens targeted by this array card are presented in Supplementary Figure S1. Samples with a cycle threshold (Ct) of less or equal to 35 were considered positive. The OROV primers and probe utilized included: Forward: 5′-TGATCCGGAGGCAGCATA-3′, Reverse: 5′-ACACCAGCATTGAGCACTTG-3′, Probe: FAM-CCGTATCTAGCTTCAAATGCC-MGB.[19] Mid turbinate swabs were tested for Influenza A, Influenza B, and SARS-CoV-2 using the CDC Influenza SARS-CoV-2 multiplex assay as described previously.[17]

OROV culture

Cellular fractions of EDTA anticoagulated blood with Ct values less than 30 were sent to the Arboviral Diseases Branch, Centers for Disease Control and Prevention for virus culture. Each sample was inoculated in volumes of 2 µl, 20 µl, and 200 µl along with 2 ml of DMEM (Gibco, Waltham, MA, USA) maintenance media supplemented with 2% fetal bovine serum (Seradign, Radnor, PA, USA) into confluent T25 flasks (Corning) of Vero cells and incubated for 1 h at 37 °C for adsorption. Eight ml of DMEM maintenance media was added to each flask and incubated at 37 °C. Flasks were visualized under light microscopy daily for the presence of cytopathic effects. When cytopathic effects impacted 50–75% of the cell monolayer the supernatant was harvested and centrifuged at 10,000 rpm for 10 min to remove cell debris. Two 0.5 ml aliquots were removed for downstream testing and the remainder was frozen as bulk.

Sequencing

Sequencing was carried out to confirm qPCR (quantitative polymerase chain reaction) diagnostics and assemble complete genomes to study the origin of the outbreak strain. In additional cases where full genomes were not available, sequencing confirmed the diagnosis in all examined cases by alignment to reference genome from strain Oropouche virus strain OROV/EC/Esmeraldas/057/2016 with GenBank accession numbers: MK506828 (M-segment), MK506823 (M-segment), and MK506818 (S-segment) using Geneious Prime (v2024.0.7).[20] Sequencing methods are available in Supplementary Methods. Oropouche genomes are available under GenBank accession numbers: PQ683506-PQ683514, PV419641-PV419661, PQ683506-PQ683508, PQ683509-PQ683511, and PQ683512-PQ683514.

Genomic analysis

All publicly available OROV sequences for the L, M, and S segments were obtained from NCBI Virus.[21] Any sequence containing more than a single unknown (e.g., N) nucleotide and/or internal gaps in the sequencing was eliminated from the analysis to avoid these unknown nucleotides biasing the analysis. Ultimately, 539 strains representing Brazil, Colombia, Ecuador, Cuba, Peru, Haiti, Panama, and Trinadad and Tobago were utilized (Supplementary Table S1) for phylogenetic comparison against Peruvian viral sequences from 2024 generated during this study. Each viral segment was processed individually for the analysis, and the sequences for each segment were aligned using the MUSCLE plugin (v5.1)[22] in Geneious Prime (v2024.0.7)[20] using the Perturbed Profile–Profile (PPP) algorithm with five hidden Markov model perturbations. Each alignment was then trimmed to make sure each sequence included the exact same number of nucleotides across identical regions to avoid bias due to extra nucleotides for some sequences. Overall, the S segment alignment was trimmed to 576 nucleotides, the M segment was trimmed to 3988 nucleotides, and

the L segment was trimmed to 6549 nucleotides, and then each of these trimmed alignments was exported as a Phylip format alignment to generate maximum likelihood trees using RAxML (v8.2.13).[23]

To determine the best model to utilize for the phylogenetic analysis, each of the alignments was tested using ModelTest-NG (v0.1.7)[24] and for each segment, it was determined that the General Time Reversible model with gamma distributed rates with estimate of proportion of invariable sites was the most appropriate for M and L segment, while the general time reversible model with site-specific evolutionary rates under the Jukes-Cantor model was used for the S segment. Maximum likelihood trees with bootstrapping (500x) were generated for each segment and then visualized and annotated using the Interactive Tree of Life (iTOL) online tool.[25] Each branch on the maximum likelihood tree was colored according to the country of isolation: (1) Brazil—orange; (2) Peru—blue; (3) Ecuador—yellow; (4) Colombia—dark blue; (5) Panama—green; (6) Haiti—cyan; (7) Cuba—dark gray; (8) Trinidad and Tobago—pink. Oropouche genomes from this study are labeled with Peru, year of isolation, and a number indicating which sample it represents between trees. Due to the large number of genomes utilized in the trees, those genomes associated with a particular clade are labeled with the country and year of isolation range to give context to the different clades of the trees.

To assess the location of amino acid differences between Oropouche strains particularly we choose one representative from each of the following: (1) isolated from Peru for this study; (2) closely related strain from Ecuador; (3) closely related strain from Colombia; (4) Brazilian outbreak; (5) 2024 Cuba strain. Amino acid alignments were conducted MUSCLE plugin (v5.1) in Geneious Prime (v2024.0.7) using the Perturbed Profile–Profile (PPP) algorithm with five hidden Markov model perturbations and the location of each amino acid differences between the representatives was marked on the alignment. A pairwise distance matrix was also constructed using Geneious Prime (v2024.0.7) for each of the genome segments.

Bayesian evolutionary analysis of Oropouche virus M segment

Evolutionary analysis was conducted on the 3988 bp of the M segment for the 539 Oropouche genomes to estimate the evolutionary clock for the different lineages of the outbreaks, and tip dates were assigned to all the sequences using the reported isolation date for each one. Temporal signal was investigated for all three genomic segments (S, M and L) with linear regression analysis of the root-to-tip distances against the sampling years using Tempest v1.5.3. Genome sequence (PP357049.1) was identified as an outlier and was removed prior to downstream analysis. Only the M segment showed sufficient temporal structure for reliable molecular clock inference (Supplementary Table S2) Model selection was performed by comparing the marginal likelihoods of six combinations of molecular clocks and coalescent models, including strict and uncorrelated relaxed clocks with the constant, exponential growth, and Bayesian SkyGrid coalescent models. Marginal likelihoods were estimated using generalized stepping-stone sampling with 50 path steps and 500,000 iterations (Supplemental Table S3). The uncorrelated relaxed clock with Bayesian SkyGrid model showed the highest marginal likelihood and was selected for subsequent analysis. Input xml files were generated using BEAUti v10.5.0.[26] The Hesegawa-Kishiro-Tayro substitution model with estimated frequencies, a gamma distribution with four categories to account for among-site rate heterogeneity, and an estimated proportion of invariant sites, were selected. The mean clock rate was assigned an informative prior at 1.3×10^{-4} substitutions per site per year. Bayesian phylogenetic inference was performed using BEAST v10.5.0.[26] Markov Chain Monte Carlo chains were run for 200 million generations, sampling every 1000 steps. Three independent Markov Chain Monte Carlo chains were run for 200 million generations using different random seeds and combined using LogCombiner after 10% burn-in removal. Convergence was assessed in Tracer v1.7.2,[27] with effective sample size (ESS) values greater than 140–200 for all parameters. TreeAnnotator v2.7.7[28] was used to generate a maximum clade credibility tree, visualized using FigTree v1.4.4 and imported into RStudio with treeio and plotted with ggtree package. The tMRCA and date estimates are reported from the MCC tree while posterior summaries are taken from the combined logs.

Ethics statement

The RIVERA study has been approved by the Institutional Review Board of Asociación Benéfica Prisma (CE0855.20) (FWA00001219), University of Virginia (FWA0006183), and Hospital Regional de Loreto. Additional approval has been obtained by the Research Commission of the Regional Health Direction of Loreto. Written informed consent was obtained for all participants.

Role of the funding source

The study sponsors had no role in the study design, collection, analysis and interpretation of data, the writing of the article, or the decision to submit it for publication.

Results

Between March 29th 2021, when the OROV target was first introduced to the diagnostic panel, and August 31st, 2024, the cutoff date for this analysis, 3985 subjects were enrolled into the RIVERA study, including 2108 AFI

cases (53.0%) and 1877 (41.1%) asymptomatic controls. Twenty AFI cases and 20 controls did not have useable OROV diagnostic results and were excluded leaving 3945 subjects–2088 cases and 1857 controls–included in this analysis (Supplementary Figure S1a).

Epidemiological and clinical profile of OROV infection

In the pre-outbreak period prior to December 1st, 2023, OROV viremia was detected in only 0.4% (13/3182) of all RIVERA subjects (6 detections in 1595 AFI cases [0.4%], 7 in 1574 [0.4%] asymptomatic controls). During the outbreak from December 1st, 2023, and August 31st, 2024, OROV was detected in 39 whole blood samples (5.0%, 32 in 455 AFI cases [7.0%], 7 in 269 [2.6%] asymptomatic controls) out of 724 samples processed in that same time frame (Fig. 1). At the epidemic peak during the first three months of 2024, an overall detection rate of 8.6% (29 detections in 339 samples) was recorded, representing a more than 20-fold increase in OROV-positivity compared with pre-outbreak levels as delineated by the prevalence over 32 months of surveillance. OROV was detected in asymptomatic individuals before and during the epidemic. Co-detection of OROV with Dengue, Histoplasma, and *M. tuberculosis*, was observed in one asymptomatic subject each, while two cases each of OROV/SARS-CoV-2 and OROV/influenza A co-detection were detected in AFI cases. No deaths were associated with the detected acute clinical illnesses, no cases of meningoencephalitis were observed, and all cases had clinically recovered from their illnesses with no sequelae when evaluated at the 28-day follow-up visit.

Clinical symptoms and their associations with OROV-positive AFI cases (excluding controls) are reported in Table 1. Several such features of illness were identified as significantly more common in OROV-positive febrile cases compared with unattributed AFI. These symptoms included joint pain (33/38 = 86.8% v 999/2050 = 48.7%), $p < 0.0001$), myalgias (35/38 = 92.1% v 1367/2050 = 66.7%, $p < 0.0001$, malaise (27/38 = 71.1% v 1076/2050 = 52.5%, $p = 0.032$) and dysuria (6/38 = 15.0% v 124/2050 = 6.0%, $p = 0.028$). Subjects with febrile illness and OROV had a higher BMI (28.2 v 25.9 kg/m^2, $p = 0.0026$) and weight (71.2 v 65.0 kg, $p = 0.0053$) than those with fever not attributed to OROV.

Viral culture

Four specimens with cycle threshold (Ct) of <30 were cultured. Three of these yielded a cytopathic virus confirmed as OROV by sequencing. The cytopathic effect was first observed in the three samples two days post inoculation, by day 3 flasks were ready to harvest.

Sequencing and genomic analysis of OROV strains

Complete genomes were assembled from 10 unique subjects. Phylogenetic analysis was performed separately for S, M, and L segments. Unrooted maximum likelihood trees were constructed, showing similar patterns for all segments including the M segment (Fig. 2), L segment (Supplementary Figure S2), and S segment (Supplementary Figure S3). The sequenced 2023–2024 Iquitos isolates were highly homogeneous among the 10 sequenced strains. They were closely related to strains sequenced in Colombia in 2024 and more distantly related to strains from Ecuador in 2016, followed by strains from Peru between 1998 and 2008, Panama in 1989, Peru between 1992 and 2000, Brazil in 1991, Brazil in 2009, and Haiti in 2014. Another cluster included a variety of historical strains from Brazil isolated between 1960 and 2023, a strain from Trinidad and Tobago isolated in 1955, and two strains from Panama isolated in 1989 and 1999. The remaining strains analyzed for comparison were from the concurrent Brazil outbreak or clustered with genomes from this outbreak. The first was a strain from Southern Peru in the Madre de Dios region bordering on Acer (indicated as PP966978.1). The other strain to cluster in this set of isolates is a strain from a traveler returning to

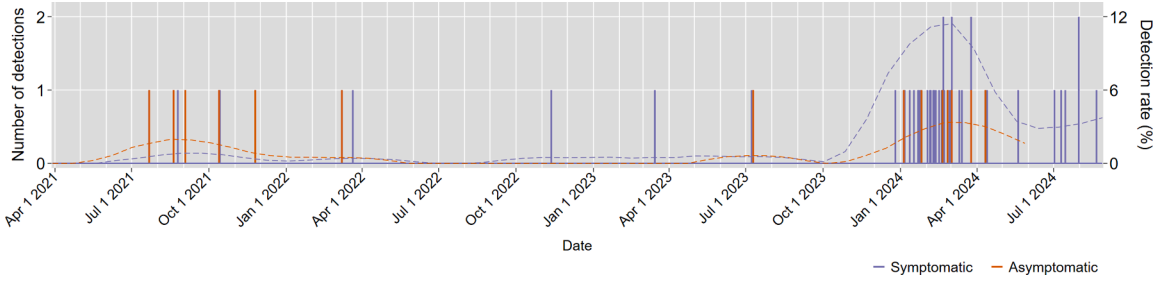

Fig. 1: Time series graph of OROV detections in symptomatic and asymptomatic RIVERA subjects over the three year study period reveal sporadic detections (displayed here as a needleplot) of Oropouche in 0.4% of cases and control prior to December 2023. Between December 2023 and August 2024, Oropouche identification increased to a peak prevalence of 11% in those with acute febrile illness and 3% of asymptomatic controls in March 2024 (prevalence of OROV among cases and controls are indicated by dashed lines with units indicated on the right axis).

	OROV-positive AFI cases		OROV-negative AFI cases		Total		Fishers' exact p
	N	%	N	%	N	%	
Total subjects	38	100.0%	2050	100.0%	2088	100.0%	–
Baseline characteristics:							
Age group							
10–24 yrs	7	18.4%	672	32.8%	1248	59.8%	0.13
25–49 yrs	24	63.2%	1001	48.8%	1984	95.0%	
≥50 yrs	7	18.4%	377	18.4%	713	34.1%	
Sex							
Male	20	52.6%	828	40.4%	1343	64.3%	0.14
Female	18	47.4%	1218	59.4%	2598	124.4%	
Residence							
Mazan and rural areas	6	15.8%	324	15.8%	635	30.4%	1.00
Iquitos Metropolitan Area	32	84.2%	1723	84.0%	3306	158.3%	
Timing of diagnosis							
Prior to 2023–24 outbreak	6	15.8%	1595	77.8%	3182	152.4%	<0.0001
During 2023–24 outbreak	32	84.2%	455	22.2%	763	36.5%	
Travel history (past 15 days)							
No travel	31	81.6%	1820	88.8%	3662	175.4%	0.18
Had traveled	7	18.4%	221	10.8%	272	13.0%	
Baseline clinical assessment							
Medical history							
Currently pregnant	0	0.0%	16	0.8%	16	0.8%	1.00
Diabetes	1	2.6%	65	3.2%	66	3.2%	1.00
HIV positive	0	0.0%	1	0.0%	1	0.0%	1.00
Hypertension	2	5.3%	50	2.4%	52	2.5%	0.25
Liver condition	0	0.0%	7	0.3%	7	0.3%	1.00
Chronic lung condition	0	0.0%	2	0.1%	2	0.1%	1.00
Renal condition	1	2.6%	18	0.9%	19	0.9%	0.30
History of heart attack	0	0.0%	0	0.0%	0	0.0%	–
History of heart failure	0	0.0%	6	0.3%	6	0.3%	1.00
History of stroke	0	0.0%	6	0.3%	6	0.3%	1.00
History of tuberculosis	0	0.0%	4	0.2%	4	0.2%	1.00
Recent antibiotic use	1	2.6%	148	7.2%	149	7.1%	0.52
Signs and symptoms (past two weeks)							
Fever	38	100.0%	2021	98.6%	2059	98.6%	1.00
Dry cough	7	18.4%	608	29.7%	615	29.5%	0.17
Productive cough	1	2.6%	412	20.1%	413	19.8%	0.0088
Cough with blood (hemoptysis)	0	0.0%	75	3.7%	75	3.6%	0.41
Sore throat	13	34.2%	747	36.4%	760	36.4%	0.87
Runny nose (rhinorrea)	9	23.7%	636	31.0%	645	30.9%	0.47
Chest pain	17	44.7%	619	30.2%	636	30.5%	0.07
Tiredness/malaise	27	71.1%	1076	52.5%	1103	52.8%	0.032
Muscle pain (myalgia)	35	92.1%	1367	66.7%	1402	67.1%	0.0007
Joint pain (arthralgia)	33	86.8%	999	48.7%	1032	49.4%	<0.0001
Loss of taste (ageusia)	9	23.7%	434	21.2%	443	21.2%	0.70
Loss of small (anosmia)	7	18.4%	267	13.0%	274	13.1%	0.33
Headache	35	92.1%	1667	81.3%	1702	81.5%	0.13
Altered consciousness/confusion	1	2.6%	37	1.8%	38	1.8%	0.51
Seizures	0	0.0%	26	1.3%	26	1.2%	1.00
Earache	3	7.9%	123	6.0%	126	6.0%	0.51
Abdominal pain	14	36.8%	658	32.1%	672	32.2%	0.60
Nausea	16	42.1%	794	38.7%	810	38.8%	0.74
Vomiting	6	15.8%	387	18.9%	393	18.8%	0.84
Diarrhea	5	13.2%	472	23.0%	477	22.8%	0.22
Bloody diarrhea (dysentry)	1	2.6%	31	1.5%	32	1.5%	0.45
Constipation	1	2.6%	145	7.1%	146	7.0%	0.52

(Table 1 continues on next page)

	OROV-positive AFI cases		OROV-negative AFI cases		Total		Fishers' exact p
	N	%	N	%	N	%	
(Continued from previous page)							
Bruising (hematomas)	0	0.0%	19	0.9%	19	0.9%	1.00
Skin lesions	0	0.0%	7	0.3%	7	0.3%	1.00
Inability to urinate (anuria)	0	0.0%	21	1.0%	21	1.0%	1.00
Difficulty or pain urinating (dysuria)	6	15.8%	124	6.0%	130	6.2%	0.028
Shortness of breath (dyspnea)	2	5.3%	114	5.6%	116	5.6%	1.00
Wheezing	0	0.0%	18	0.9%	18	0.9%	1.00
Intercostal retractions	0	0.0%	14	0.7%	14	0.7%	1.00
Conjunctivitis	0	0.0%	30	1.5%	30	1.4%	1.00
Rashes	1	2.6%	52	2.5%	53	2.5%	1.00
Adenopathy	1	2.6%	14	0.7%	15	0.7%	0.24
Intracerebral hemorrhage	0	0.0%	8	0.4%	8	0.4%	1.00
Ischemic stroke	0	0.0%	15	0.7%	15	0.7%	1.00
Redness of the conjunctiva	0	0.0%	44	2.1%	44	2.1%	1.00
Jaundice	0	0.0%	31	1.5%	31	1.5%	1.00
Hemoptysis	0.00	0.00	16.00	0.01	16.00	0.01	1.00
Vital signs and anthropometry	Mean	SD	Mean	SD	Mean	SD	t-test p
Temperature (C)	38.54	0.37	38.45	0.67	38.45	0.66	0.44
Heart rate (BPM)	95.37	18.52	90.05	20.36	90.14	20.34	0.11
Respiratory rate (BPM)	19.17	2.12	19.09	4.94	19.09	4.90	0.93
Oxygen saturation (%)	98.14	0.81	97.94	1.11	97.94	1.10	0.27
Systolic blood pressure (mmHg)	105.05	18.47	108.09	17.91	108.03	17.92	0.31
Diastolic blood pressure (mmHg)	66.00	7.81	67.51	14.71	67.48	14.61	0.533
Height (cm)	158.84	9.64	158.19	8.57	158.21	8.59	0.64
Weight (kg)	71.21	14.15	65.02	13.53	65.13	13.57	0.0053
Body Mass Index (kg/m2)	28.19	5.01	25.89	4.65	25.93	4.66	0.0026

Individuals with OROV were less likely than individuals undifferentiated acute febrile illness to have productive cough or chest pain, but more likely to have malaise, arthralgia, myalgia, and dysuria. The prevalence of OROV in individuals with AFI was not greater in either sex or in the examined age categories or with pre-existing illness relative to that observed in undifferentiated acute febrile illness. The prevalence of OROV was higher in individuals who had a greater body weight or body mass index was compared with individuals presenting with acute febrile illnesses of other etiologies.

Table 1: **Descriptive comparison of the prevalence signs and symptoms of illness in individuals presenting with acute febrile illness associated with OROV and all other causes of acute febrile illness.**

Italy from Cuba (indicated as PQ363069.1). The high bootstrap values express high certainty in the segregation of isolates in the visualized clades.

To examine the genomic regions exhibiting amino acid differences between different geographic origins, amino acid alignments for a representative genome of a Peruvian strain from this study, the two phylogenetically closest countries (Colombia and Ecuador), and the 2023–24 outbreak (Brazil and Cuba) for each of the three genomic segments (Fig. 3). A single polymorphism was identified in the S segment and minimal polymorphisms in the L segments, while polymorphisms were concentrated in the N terminus of the Gc protein on the M segment. Pairwise distance matrices of amino acid sequences for the different segments of the genome between the representatives' genomes further supported these conclusions. All the S segments were identical, except for the Peruvian genome isolated in 1992 (99.5% pairwise identity) and the L segment ranged from 98.2% to 99.7% pairwise identity, but the M segment ranged from 91.6% to 99.9% pairwise identity between the all the strains (Fig. 3D and E and F).

Bayesian evolutionary analysis of 538 Oropouche M segments demonstrated that the 2023–24 Brazilian outbreak lineage separated from the 2023–24 Peruvian outbreak lineage in 1797 (95% Highest Posterior Density (HPD): 1556–1947) along with the 2024 Colombian strain and 2016 Ecuadorian strains. The 2023–24 Peruvian outbreak strains then evolved away from the 2016 Ecuadorian strains in 2011 (95% HPD: 2008–-2014) and the Colombian strain in 2016 (95% HPD: 2012–2019) (Fig. 4).

Discussion

The RIVERA study demonstrated the ability of health facility-based surveillance to rapidly detect an ongoing outbreak of an emerging zoonotic virus in the Amazonian region and inform genomic epidemiology in response. Surveillance was calibrated to sample 100 samples a month, an intensity that would allow for the

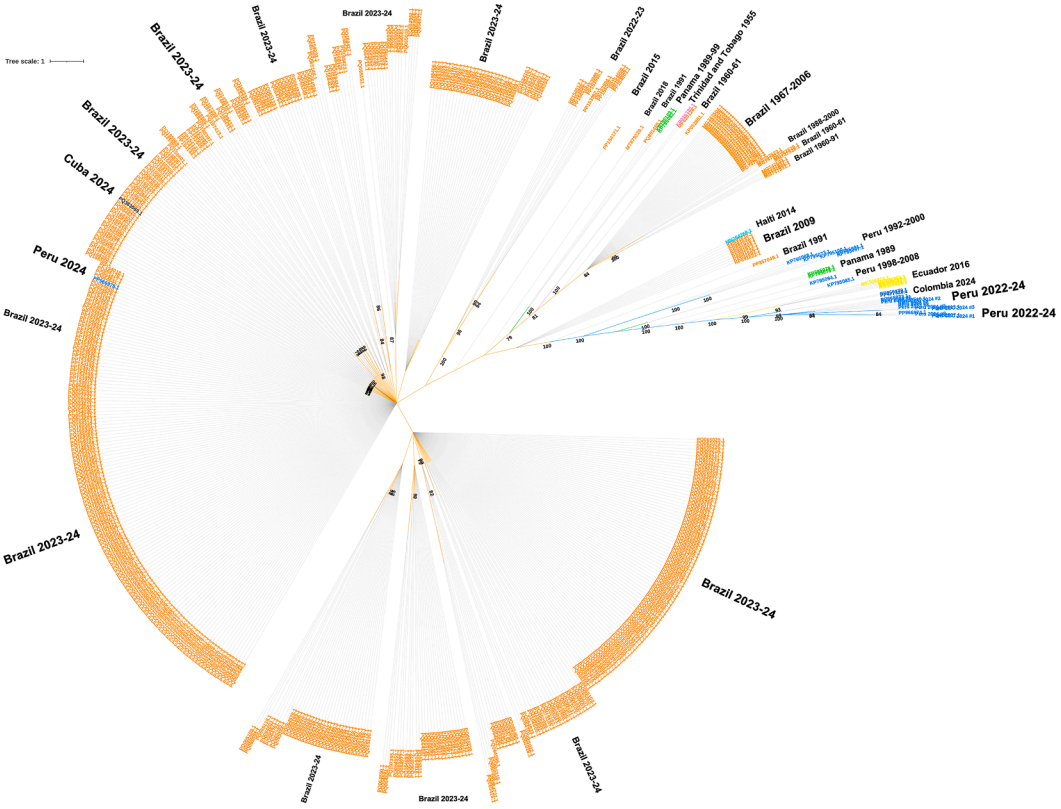

Fig. 2: Unrooted Maximum-likelihood (ML) tree of 539 Oropouche genomes based on the 3988 bp of the M segment. Tree was generated using the General Time Reversible model with gamma distributed rates with estimate of proportion of invariable sites and bootstrapped 500 times with displayed bootstrap values between 75 and 100. Nodes and branches are colored based on country of isolation including: (1) Brazil—orange; (2) Peru—blue; (3) Ecuador—yellow; (4) Colombia—dark blue; (5) Panama—green; (6) Haiti—cyan; (7) Cuba—dark gray; (8) Trinidad and Tobago—pink. Tree scale indicates number of substitutions per distance of branch.

detection of a fivefold change in the monthly prevalence of a pathogen with a baseline prevalence of 1%, assuming an 80% power and 95% confidence level. This allowed the ascertainment of the time of onset of the outbreak and the comparison of the previously circulating endemic viruses in the local area to those obtained during the outbreak in 2023–2024 and with other OROV sequences publicly available from different geospatial origins in South America. The case–control design of the parent study allowed for the identification of asymptomatic transmission. Risk factors associated with an increased prevalence of infection with OROV among individuals with acute febrile illness was a greater weight and body mass index (BMI). Obesity has been linked to a heightened risk of infection, poor clinical outcomes, and elevated viral shedding in various viral diseases, including other arboviral infections.[29] The underlying mechanisms driving poor clinical outcomes may involve the role of adipose tissue in viral pathogenesis, and an overall downregulation of the immune system often observed in individuals with chronic illnesses.[30] However, given the relative small number of cases in this series, these findings should be considered is preliminary and validated in larger studies.

Despite a large outbreak in Brazil occurring concurrently, sequencing of virus samples from Iquitos revealed that the circulating OROV strains there were more closely related to those from outbreaks in Colombia (2020) and Ecuador (2016), both of which are thought to have originated in Peru. The N terminus of the Gc protein is the coding region for the antigen that appears to drive protective immunity based on the work of Hellert[31] and Gutierrez.[32] Alignment and comparisons of the amino acids of the M segment reveal an 8.88% divergence in amino acids in the variable regions of the Gc protein that represents the head of the spike protein between the 2023 Brazil strains and the strains we identified from Peru in late 2023 and early 2024. The findings are of importance as they suggest that environmental factors have favored the transmission of OROV across the Amazon, but that the epidemic in Peru has a distinct ancestry and does not represent a geographic extension of OROV from Brazil, despite

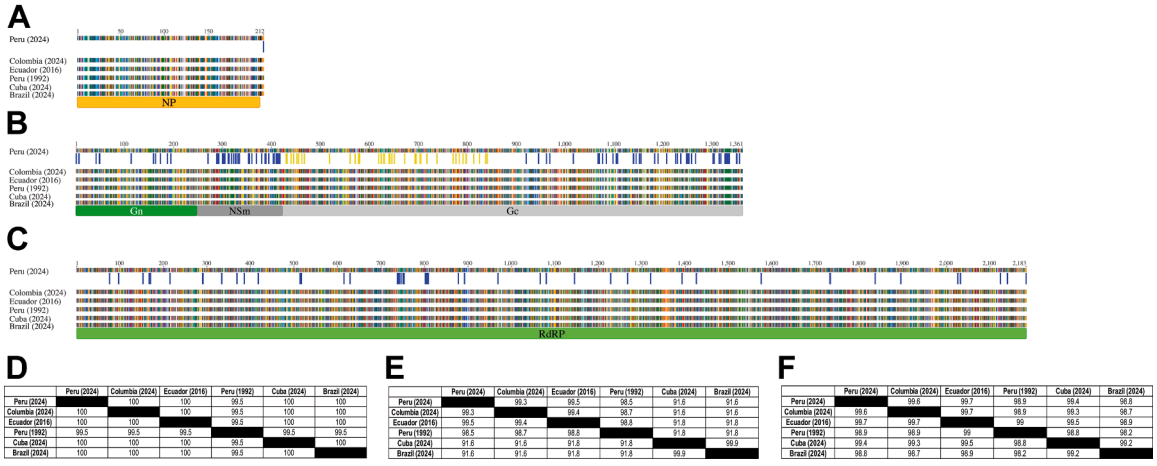

D	Peru (2024)	Columbia (2024)	Ecuador (2016)	Peru (1992)	Cuba (2024)	Brazil (2024)
Peru (2024)		100	100	99.5	100	100
Columbia (2024)	100		100	99.5	100	100
Ecuador (2016)	100	100		99.5	100	100
Peru (1992)	99.5	99.5	99.5		99.5	99.5
Cuba (2024)	100	100	100	99.5		100
Brazil (2024)	100	100	100	99.5	100	

E	Peru (2024)	Columbia (2024)	Ecuador (2016)	Peru (1992)	Cuba (2024)	Brazil (2024)
Peru (2024)		99.3	99.5	98.5	91.6	91.6
Columbia (2024)	99.3		99.4	98.7	91.6	91.6
Ecuador (2016)	99.5	99.4		98.8	91.8	91.8
Peru (1992)	98.5	98.7	98.8		91.8	91.8
Cuba (2024)	91.6	91.6	91.8	91.8		99.9
Brazil (2024)	91.8	91.6	91.8	91.8	99.9	

F	Peru (2024)	Columbia (2024)	Ecuador (2016)	Peru (1992)	Cuba (2024)	Brazil (2024)
Peru (2024)		99.6	99.7	98.9	99.4	98.8
Columbia (2024)	99.6		99.7	98.9	99.3	98.7
Ecuador (2016)	99.7	99.7		99	99.5	98.9
Peru (1992)	98.9	98.9	99		98.8	98.2
Cuba (2024)	99.4	99.3	99.5	98.8		99.2
Brazil (2024)	98.8	98.7	98.9	98.2	99.2	

Fig. 3: Amino acid sequence alignment for the S (A), M (B), and L (C) segments of the Oropouche virus from Peru (2024), Colombia (2024), Ecuador (2016), Peru (1992), Cuba (2024), and Brazil (2024). The S segment has 1/212 (0.47%) amino acid heterogeneity and the L segment 52/2183 (2.38%) amino acid heterogeneity among the viruses from different countries. However, there is quite a significant amount of amino acid heterogeneity in the M segment, as it has 127/1361 (9.33%) amino acid heterogeneity including 38/428 (8.88%) amino acid changes in the N terminus of Gc, the region coding the antigen that is purported to mediate protective immunity. Pairwise distance matrices for the S (D), M (E), and L (F) segments of the Oropouche virus from Peru (2024), Colombia (2024), Ecuador (2016), Peru (1992), Cuba (2024), and Brazil (2024) based on amino acid sequences. NP- nucleoprotein; Gn-viral surface glycoprotein Gn; NSm, non-structural protein Sm; Gc viral surface glycoprotein Gc; RdRP, RNA-dependent RNA polymerase.

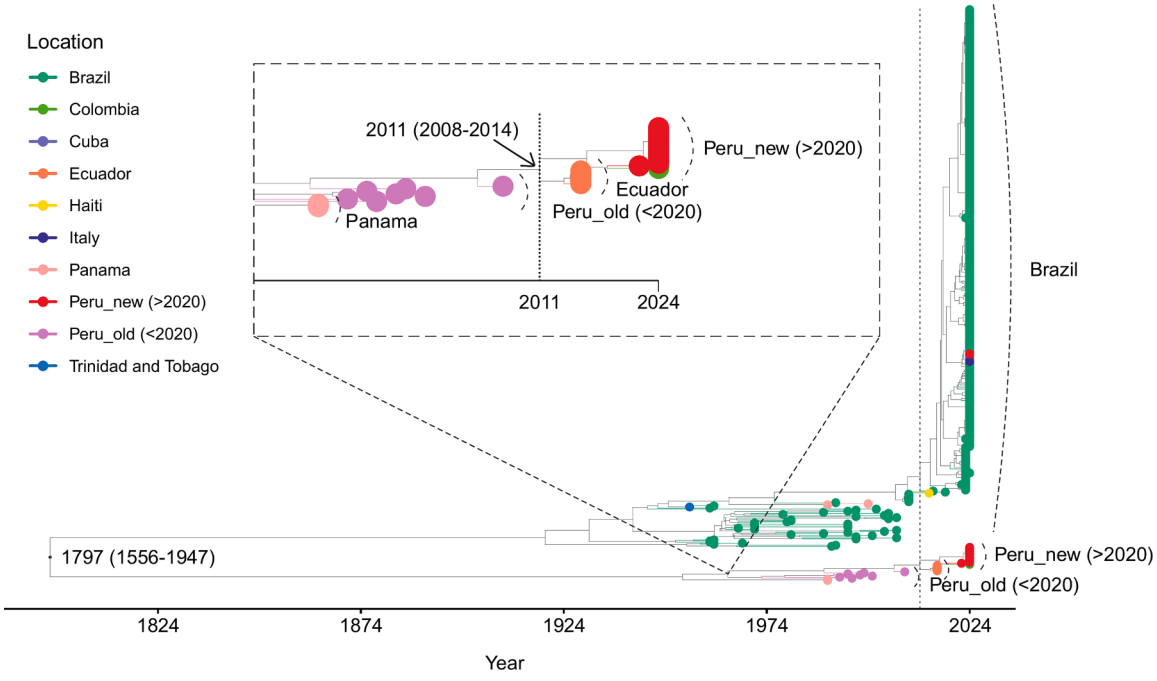

Fig. 4: Bayesian maximum clade credibility (MCC) phylogenetic tree representing the M segment for 538 Oropouche viral strains isolated across the world over a 70-year period, which demonstrates the separation of the 2023–24 Brazilian outbreak lineage from the 2023–24 Peruvian lineage in 1797 (95% HPD: 1556–1947). Tips are labeled with the country and year of isolation and are also colored based on country of isolation including: (1) Brazil—green; (2) Peru_new (>2020)—red; (3) Ecuador—orange; (4) Colombia—light green; (5) Panama—pink; (6) Haiti—yellow; (7) Trinidad and Tobago—pale blue.

daily barges traveling along the Amazon River between Manaus and Iquitos and a predicted multitude of introductions from human communities traveling in each direction. This observation is supported by a phylogenetic analysis the incudes all publicly available sequences associated with specimen source, location, and date that shows that the last common ancestor of outbreak strains from Peru and Brazil was in 1797, and that OROV from Peru diverged from available Ecuadorian isolates in 2011 and Colombian isolates in 2016. Given these ample opportunities for the introduction of Brazilian OROV strains to Peru during this two-year outbreak, we speculate that neutralizing antibodies to the Brazil strain exist in the Peruvian population. The epidemiology of OROV is understudied, but annual seroprevalence surveys in the region have previously documented annual seroconversion rates of 28% in rural communities within 10 km of Iquitos in the absence of an outbreak, strongly suggesting that background transmission in the area is both intense and continuous.[33] This study demonstrates the importance of incorporating genomic epidemiology of infectious agents across countries and available databases to improve the understanding of the transmission dynamics of emerging infectious diseases.

Newly emerging pathogenic orthobunyaviruses have been detected in the Amazonian region and have been associated with genome segment reassortment.[34] Such is the case of Iquitos virus, which is a product of the reassortment of the S and L segments of OROV and the M segment of an unknown Simbu serogroup virus.[5] Other human pathogenic orthobunyaviruses including Itaya[8] and Bellavista[9] viruses have been identified in the region of Loreto, suggesting that this area is a hotspot for transmission. The sylvatic cycle of OROV, and its role in the spillover of orthobunyaviruses into the urban cycle of disease transmission remains poorly studied. OROV has been isolated from sloths, non-human neotropical primates, and a rodent, and seropositivity has been detected in a variety of wild and domestic birds.[3] It is critically important to understand the role of arthropods and other species of insects in the transmission of OROV from birds to humans. Direct evidence of larger wild mammalian species in OROV transmission is negligible as there is a limited interface between these animals and human populations and insufficient study of isolated viruses from animal reservoirs. Additionally, seropositivity to OROV in domestic chickens and ducks, previously demonstrated in an outbreak investigation in Brazil,[3] would open the possibility of a domestic animal reservoir within urban areas where small-scale poultry rearing is widely practiced. Therefore, an important future direction for research would be to establish a human cohort to be sampled concurrently alongside arthropods, mosquitoes, avian and mammalian species from the same location. This would provide a unique evidence base to characterize the transmission dynamics of OROV.

Contributors

Conceptualization: MPO, FS, PPY, JL, ERH, MNK.
Methodology: MPO, PPY, JMC, CRA, CVM, ERH, MNK, EM, BP, CTP.
Software: KKC, JC, ERH, CTP, EM, BP.
Validation: JCM, FS, ERH, EM, BP, CTP, ACB, HRH, MNK.
Formal Analysis: FS, JMC, PFGB, HRH, EM, BP, KKC, CTP, MNK.
Investigation: MPO, FS, WVSL, TNPV, PFGB, CRA, YAAP, JL, KKC, CTP, HRH, ED, BJR, ACB.
Resources: MPO, MNK, FS, CTP, ACB, PPY.
Data Curation: PPY, JMC, CTP, PFGB, MPO, MNK.
Writing (original draft): MPO, FS, JMC, HRH, ED, ACB, KKC, CTP, MNK.
Writing (review and editing): MPO, FS, PPY, JMC, EM, WVSL, TNPV, PFGB, TGF, CRA, HRH, ED, BJR, AAB, YAAP, CVM, JL, ERH, BP, KKC, CTP, MNK.
Visualization: KKC, CTP, FS, EM, BP.
Supervision: MPO, FS, PPY, PGB, ACB, YAP, CVM, CRA.
Project Acquisition: MPO, MNK.
Funding Acquisition: MPO, MNK.
Decision to submit manuscript: MPO, MNK.

Data sharing statement

De-identified participant level data is available upon request with a data sharing agreement upon publication. All sequences have been deposited in public databases and strains are available for academic use by contacting the CDC's Arbovirus Reference Collection.

Declaration of interests

The authors have no competing interests to disclose.

Acknowledgements

This project is supported by the Centers for Disease Control and Prevention of the U.S. Department of Health and Human Services (HHS) as part of a cooperative agreement award with CDC/HHS, award number U01GH002270 to MNK. Additional training and capacity-building support was obtained through the National Institutes of Health/Fogarty International Center (D43TW010913 to MNK; K43TW012298 to FS), the National Institutes of Health/National Institute for Allergies and Infectious Diseases (K01AI168493 to JMC), the Infectious Diseases Training Program 5T32AI007046-48 and the Division of Infectious Diseases and The Division of Infectious Diseases and International Health of the University of Virginia. The study sponsors had no role in the study design, collection, analysis and interpretation of data, the writing of the article, or the decision to submit it for publication. The findings and conclusions in this report are those of the authors and do not necessarily represent the official position of the U.S. Centers for Disease Control and Prevention. The communicating author has full access to all data and accepts responsibility for data and research integrity of the findings presented in the manuscript.

Appendix A. Supplementary data

Supplementary data related to this article can be found at https://doi.org/10.1016/j.lana.2026.101413.

References

1 Sakkas H, Bozidis P, Franks A, Papadopoulou C. Oropouche fever: a review. *Viruses*. 2018;10:175.
2 Wesselmann KM, Postigo-Hidalgo I, Pezzi L, et al. Emergence of Oropouche fever in Latin America: a narrative review. *Lancet Infect Dis*. 2024;24:e439–e452.
3 Pinheiro FP, Travassos da Rosa AP, Travassos da Rosa JF, Bensabath G. An outbreak of Oropouche virus diease in the vicinity of santarem, Para, Barzil. *Tropenmed Parasitol*. 1976;27:213–223.

4 Borborema CA, Pinheiro FP, Albuquerque BC, da Rosa AP, da Rosa JF, Dourado HV. [1st occurrence of outbreaks caused by Oropouche virus in the State of Amazonas]. *Rev Inst Med Trop Sao Paulo*. 1982;24:132–139.
5 Aguilar PV, Barrett AD, Saeed MF, et al. Iquitos virus: a novel reassortant Orthobunyavirus associated with human illness in Peru. *PLoS Negl Trop Dis*. 2011;5:e1315.
6 Navarro J-C, Giambalvo D, Hernandez R, et al. Isolation of Madre de Dios Virus (Orthobunyavirus; Bunyaviridae), an Oropouche Virus Species Reassortant, from a Monkey in Venezuela. *Am J Trop Med Hyg*. 2016;95:328–338.
7 Tilston-Lunel NL, Shi X, Elliott RM, Acrani GO. The potential for reassortment between Oropouche and Schmallenberg orthobunyaviruses. *Viruses*. 2017;9:220.
8 Hontz RD, Guevara C, Halsey ES, et al. Itaya virus, a novel orthobunyavirus associated with human febrile illness, Peru. *Emerg Infect Dis*. 2015;21:781–788.
9 Hang J, Yang Y, Kuschner RA, et al. Genome sequence of Bellavista virus, a novel orthobunyavirus isolated from a pool of mosquitoes captured near iquitos, Peru. *Genome Announc*. 2016;4:e01262-16.
10 Gallichotte EN, Ebel GD, Carlson CJ. Vector competence for Oropouche virus: a systematic review of pre-2024 experiments. *PLoS Negl Trop Dis*. 2025;19:e0013014.
11 McGregor BL, Connelly CR, Kenney JL. Infection, dissemination, and transmission potential of north American Culex quinquefasciatus, Culex tarsalis, and culicoides sonorensis for Oropouche virus. *Viruses*. 2021;13:226.
12 Bastos MS, Figueiredo LTM, Naveca FG, et al. Identification of Oropouche Orthobunyavirus in the cerebrospinal fluid of three patients in the Amazonas, Brazil. *Am J Trop Med Hyg*. 2012;86:732–735.
13 Lorenz C, Azevedo TS, Virginio F, Aguiar BS, Chiaravalloti-Neto F, Suesdek L. Impact of environmental factors on neglected emerging arboviral diseases. *PLoS Negl Trop Dis*. 2017;11:e0005959.
14 Sciancalepore S, Schneider MC, Kim J, Galan DI, Riviere-Cinnamond A. Presence and multi-species spatial distribution of Oropouche virus in Brazil within the one health framework. *Trop Med Infect Dis*. 2022;7:111.
15 Pan American Health Organization. *Oropouche*. ARBO Portal; 2025. https://www.paho.org/es/arbo-portal/arbo-portal-oropouche. Accessed June 6, 2025.
16 Pan American Health Organization. Public health risk assessment related to Oropouche virus (OROV) in the region of the Americas. https://www.paho.org/en/documents/public-health-risk-assessment-related-oropouche-virus-orov-region-americas-3-august-2024; 2024. Accessed June 6, 2025.
17 Peñataro Yori P, Paredes Olórtegui M, Schiaffino F, et al. Etiology of acute febrile illness in the peruvian amazon as determined by modular formatted quantitative PCR: a protocol for RIVERA, a health facility-based case-control study. *BMC Public Health*. 2023;23:674.
18 Forshey BM, Guevara C, Laguna-Torres VA, et al. Arboviral etiologies of acute febrile illnesses in Western South America, 2000-2007. *PLoS Negl Trop Dis*. 2010;4:e787.
19 Rainey JJ, Siesel C, Guo X, et al. Etiology of acute febrile illnesses in Southern China: findings from a two-year sentinel surveillance project, 2017-2019. *PLoS One*. 2022;17:e0270586.
20 Kearse M, Moir R, Wilson A, et al. Geneious Basic: an integrated and extendable desktop software platform for the organization and analysis of sequence data. *Bioinformatics*. 2012;28:1647–1649.
21 For Biotechnology Information. NCBI Virus: community portal for viral sequence data from RefSeq, GenBank and other NCBI repositories. NCBI Virus: Sequences for Discovery. https://www.ncbi.nlm.nih.gov/labs/virus/vssi/#/. Accessed June 6, 2025.
22 Edgar RC. Muscle5: High-accuracy alignment ensembles enable unbiased assessments of sequence homology and phylogeny. *Nat Commun*. 2022;13:6968.
23 Stamatakis A. RAxML version 8: a tool for phylogenetic analysis and post-analysis of large phylogenies. *Bioinformatics*. 2014;30:1312–1313.
24 Darriba D, Posada D, Kozlov AM, Stamatakis A, Morel B, Flouri T. ModelTest-NG: a new and scalable tool for the selection of DNA and protein evolutionary models. *Mol Biol Evol*. 2020;37:291–294.
25 Letunic I, Bork P. Interactive Tree of Life (iTOL) v6: recent updates to the phylogenetic tree display and annotation tool. *Nucleic Acids Res*. 2024;52:W78–W82.
26 Suchard MA, Lemey P, Baele G, Ayres DL, Drummond AJ, Rambaut A. Bayesian phylogenetic and phylodynamic data integration using BEAST 1.10. *Virus Evol*. 2018;4:vey016.
27 Rambaut A, Drummond AJ, Xie D, Baele G, Suchard MA. Posterior summarization in Bayesian phylogenetics using tracer 1.7. *Syst Biol*. 2018;67:901–904.
28 Drummond AJ, Rambaut A. BEAST: bayesian evolutionary analysis by sampling trees. *BMC Evol Biol*. 2007;7:214.
29 Hameed M, Geerling E, Pinto AK, Miraj I, Weger-Lucarelli J. Immune response to arbovirus infection in obesity. *Front Immunol*. 2022;13:968582.
30 Guglielmi V, Colangeli L, D'Adamo M, Sbraccia P. Susceptibility and severity of viral infections in obesity: lessons from influenza to COVID-19. Does leptin play a role? *Int J Mol Sci*. 2021;22:3183.
31 Hellert J, Aebischer A, Wernike K, et al. Orthobunyavirus spike architecture and recognition by neutralizing antibodies. *Nat Commun*. 2019;10:879.
32 Gutierrez B, Wise EL, Pullan ST, et al. Evolutionary dynamics of Oropouche virus in South America. *J Virol*. 2020;94:e01127-19.
33 Watts DM, Phillips I, Callahan JD, Griebenow W, Hyams KC, Hayes CG. Oropouche virus transmission in the Amazon River basin of Peru. *Am J Trop Med Hyg*. 1997;56:148–152.
34 Ladner JT, Savji N, Lofts L, et al. Genomic and phylogenetic characterization of viruses included in the Manzanilla and Oropouche species complexes of the genus Orthobunyavirus, family Bunyaviridae. *J Gen Virol*. 2014;95:1055–1066.